

(*d,p*) and (*d,t*) Reactions on Magnesium Isotopes*E. W. HAMBURGER† AND A. G. BLAIR
University of Pittsburgh, Pittsburgh, Pennsylvania

(Received February 16, 1960)

Natural and enriched magnesium targets were bombarded with 14.8-Mev deuterons from the University of Pittsburgh cyclotron. The reaction products were magnetically analyzed and detected in a scintillation counter. Angular distributions from 10° to 60° (in some cases to 90°) were obtained for most of the following reactions: $\text{Mg}^{24}(d,p)$ to the 0-, 1.61-, and 1.96-Mev levels of Mg^{25} , $\text{Mg}^{25}(d,t)$ to the 0-, 1.37-, 4.12-, 4.24-, 5.24-, 6.01-, 7.33-, and 7.60-Mev levels of Mg^{24} , and $\text{Mg}^{26}(d,t)$ to the 0-, 0.58-, 0.98-, 1.61-, 1.96-, 2.56-, 2.74-, 2.80-, 3.40-, and 3.90-Mev levels of Mg^{25} . The level at 7.60 Mev in Mg^{24} has not been reported before. The observed angular distributions are compared to stripping theory, and l values and absolute reduced widths are extracted. An anomaly in the angular distribution was found for the transitions between the Mg^{24} and Mg^{25} ground states and was studied as a function of incident deuteron energy. The reduced widths obtained are compared to the predictions of the rotational model, and, in general, good agreement is found; however, an admixture (of $\approx 15\%$) of higher rotational bands was found in the Mg^{26} ground-state wave function.

I. INTRODUCTION

THE low-lying states of nuclei with mass number 25 have been extensively studied experimentally,^{1,2} and many of the properties of these nuclei have been explained satisfactorily on the basis of the rotational model.^{2,3} Rotational properties are expected for other nuclei in this mass region as well, but the data are not so numerous and the interpretation of the spectra is not so simple as for the $A=25$ cases.

The present work was undertaken in order to obtain additional information on the magnesium nuclei. Also, since (*d,t*) reactions have not as yet been used very extensively in nuclear spectroscopy, some of our data should be valuable for purposes of a systematic study of (*d,t*) reactions.⁴ In particular, the comparison between the $\text{Mg}^{24}(d,p)\text{Mg}^{25}$ ground-state (g.s.) and the $\text{Mg}^{25}(d,t)\text{Mg}^{24}$ ground-state reactions determines a numerical factor which allows one to extract absolute stripping reduced widths from the (*d,t*) angular distributions for nuclei in this region.

Angular distributions for the $\text{Mg}^{24}(d,p)\text{Mg}^{25}$ reaction have been obtained previously by Hinds *et al.*⁵ and Holt *et al.*⁶ The $\text{Mg}^{25}(d,t)\text{Mg}^{24}$ and $\text{Mg}^{26}(d,t)\text{Mg}^{25}$ reactions have not been reported previously, although the ground-state and 1.37-Mev angular distributions

from the analogous $\text{Mg}^{25}(p,d)\text{Mg}^{24}$ reaction have been obtained.⁷

In the following sections we outline our experimental procedure, and present and discuss the results for each reaction studied.

II. EXPERIMENTAL PROCEDURE

Deuterons from the University of Pittsburgh cyclotron are magnetically focused and analyzed, producing in a shielded scattering room a $\approx 1 \mu\text{a}$, ≈ 14.8 -Mev beam, whose energy spread is ≈ 50 kev. (For details of the scattering system see Bender *et al.*⁸ and Hamburger.⁹) The reaction products produced in the target are analyzed by a magnetic spectrometer, which can be rotated about the target, and are then detected in a thin CsI(Tl) scintillator. Different reaction particles are distinguished by their different pulse heights, as determined with the aid of a 6-channel pulse-height analyzer and a 256-channel pulse-height analyzer. Detection may also be accomplished by means of a nuclear emulsion system.⁹

Although several kinds of target material were used in the present experiment, most of the work was done using self-supporting metallic magnesium foils, each with a thickness of ≈ 2 mg/cm². One of these foils was prepared by evaporating natural magnesium onto a polished stainless steel plate, then peeling off the foil;⁵ two other foils, enriched to $\approx 99\%$ in Mg^{25} and Mg^{26} , respectively, were obtained from the Oak Ridge National Laboratory.

For scattering angles greater than 6° , the deuteron beam was monitored by a Faraday cup mounted behind the target. For smaller scattering angles, the Faraday cup was removed and the beam was monitored by a scintillation counter set at an angle of $\approx 50^\circ$ to the

* Work done at Sarah Mellon Scaife Radiation Laboratory and assisted by the joint program of the Office of Naval Research and the U. S. Atomic Energy Commission.

† Now at Departamento de Física, Faculdade de Filosofia, Universidade de São Paulo, São Paulo, Brazil.

¹ P. M. Endt and C. M. Braams, *Revs. Modern Phys.* **29**, 683 (1957).

² A. E. Litherland, H. McManus, E. B. Paul, D. A. Bromley, and H. E. Gove, *Can. J. Phys.* **36**, 378 (1958).

³ A. Bohr and B. Mottelson, *Kgl. Danske Videnskab. Selskab, Mat.-fys. Medd.* **20**, No. 16 (1953).

⁴ A. I. Hamburger (to be published).

⁵ S. Hinds, R. Middleton, and G. Parry, *Proc. Phys. Soc. (London)* **71**, 49 (1958).

⁶ J. R. Holt and T. N. Marsham, *Proc. Phys. Soc. (London)* **A66**, 258 (1953).

⁷ E. F. Bennett, Ph.D. thesis, University of Princeton, 1958 (unpublished).

⁸ R. S. Bender, E. M. Reilley, A. J. Allen, R. Ely, J. S. Arthur, and H. J. Hausman, *Rev. Sci. Instr.* **23**, 542 (1952).

⁹ E. W. Hamburger, Ph.D. thesis, University of Pittsburgh, 1959 (unpublished).

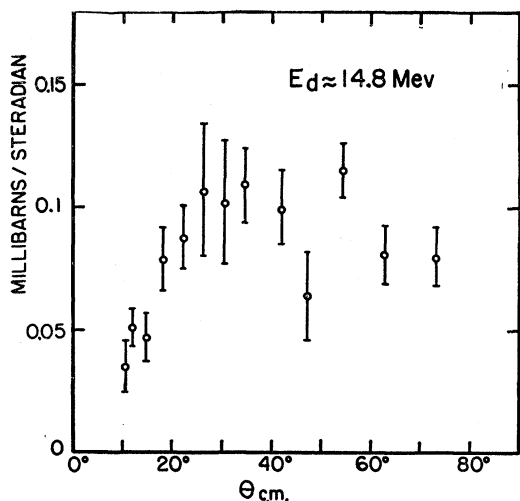


FIG. 1. Angular distribution for the $\text{Mg}^{24}(d,p)\text{Mg}^{25}$ 1.61-Mev reaction. The error bars indicate estimated upper limits on the errors. If the level is $\frac{7}{2}^+$ only $l=4$ is allowed. The slope below 30° cannot be fitted by $l=4$ Butler curves. Only $l=3$, with $r_0=6f$, fits this slope; with this fit, $(2J+1)\theta^2=0.03$, and the level would have negative parity.

direction of the incident beam. The latter monitor system introduced an estimated uncertainty of 10% in the small angle data (see Fig. 3).

In the angular distribution plots shown, the uncertainty in the relative cross sections other than the statistical error is estimated to be less than $\pm 10\%$. The absolute cross section scales (given in the c.m. system) in the figures are estimated to be accurate to

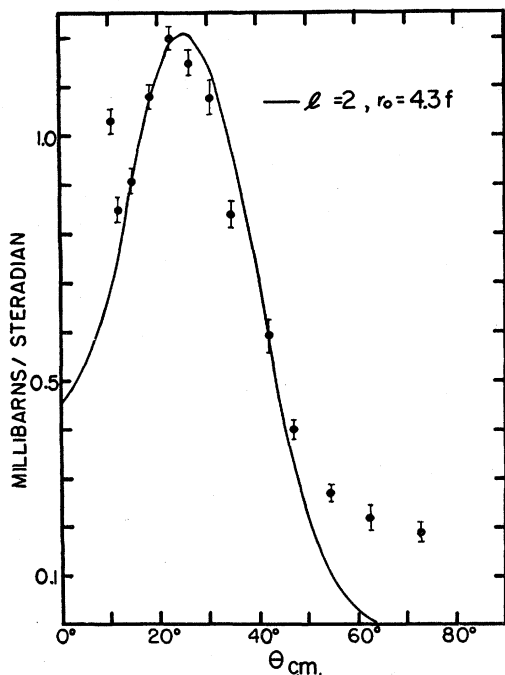


FIG. 2. Angular distribution for the $\text{Mg}^{24}(d,p)\text{Mg}^{25}$ 1.96-Mev reaction. The errors shown are statistical.

within $\pm 25\%$. These scales were obtained by comparing the $\text{Mg}^{24}(d,p)\text{Mg}^{25}$ ground-state cross section with the $\text{C}^{12}(d,p)\text{C}^{13}$ g.s. cross section (both at ≈ 14.8 -Mev incident deuteron energy) using carefully weighed targets of magnesium and polyethylene. The above carbon cross section has been measured recently to be $15.5 \pm 20\%$ millibarns per steradian at the peak of its angular distribution.¹⁰

The angular spread of the incident beam and of the particles accepted by the detector was $\approx 1^\circ$. The direction of the incident beam and the scattering angles were known to within $\pm 0.5^\circ$.

III. $\text{Mg}^{24}(d,p)\text{Mg}^{25}$ REACTION

Because this reaction already has been carefully studied⁵ (with deuteron energy of 8.9 Mev), angular distributions of only a few states were obtained in the present experiment. We studied the Mg^{25} g.s. in order to compare it with the $\text{Mg}^{25}(d,t)\text{Mg}^{24}$ g.s. reaction, the 1.61-Mev level because it did not show a stripping pattern at $E_d=8.9$ Mev,⁵ and the 1.96-Mev level. The three angular distributions are shown in Figs. 1, 2, and 3. Table I gives the reduced widths obtained from a fit of stripping curves to the distributions.

A. Mg^{25} 1.61-Mev Level

The angular distribution for the 1.61-Mev level looks quite different from that obtained at $E_d=8.9$ Mev,⁵ but neither can be fitted by a stripping curve. By analogy with the 1.61-Mev level in the mirror nucleus Al^{25} , the present level should have a spin and parity of $\frac{7}{2}^+$, in which case only $l=4$ stripping would be allowed by conservation of angular momentum and parity.¹¹ An $l=4$ curve does not fit the slope of the distribution on the small-angle side; this slope can be fitted with an $l=3$ curve only (which would imply $\frac{5}{2}^-$ or $\frac{7}{2}^-$ as the spin and parity of this state), but even such a curve does not fit the $\theta > 30^\circ$ region. If the level is $\frac{7}{2}^+$, however, it could be assigned to the rotational band based on the intrinsic configuration of the ground state (see Fig. 11), so that the odd neutron would be in a state of orbital angular momentum $l=2$. In this case, no stripping should be seen, since it can proceed only by $l=4$ for the transferred neutron; the relatively small cross section found for this level is consistent with such an explanation.

B. Mg^{25} 1.96-Mev Level

The angular distribution for this level, which is well known to have a spin and parity of $\frac{5}{2}^+$, can be fitted well with a Butler curve having $l=2$, in agreement with the $E_d=8.9$ -Mev data. The reduced width is $\theta^2=0.0031$,

¹⁰ S. Mayo and E. W. Hamburger, Appendix A in reference 9.

¹¹ A $\frac{7}{2}^+$ level could be reached by neutron capture with $l=2$ by means of spin-flip. We have not attempted to fit a spin-flip curve to the present data. For treatments of spin-flip, see reference 13 and 14.

again in reasonable agreement with the value of $\theta^2=0.0043$ extracted from the data of Hinds *et al.*⁵ by Macfarlane and French.¹²

C. Mg^{25} Ground State

a. Results at $E_d=14.8$ Mev

An $l=2$ stripping curve fits the data of Fig. 3 only in the region $20^\circ < \theta_{\text{c.m.}} < 40^\circ$; below 20° the experimental distribution continues to rise while the theoretical curve drops sharply. The data suggest a mixture of $l=0$ and $l=2$ and can, in fact, be fitted with such a mixture if one takes $\theta^2(l=2) \approx 8\theta^2(l=0)$. However, the spins and parities of the Mg^{24} and Mg^{25} ground states are known to be 0^+ and $\frac{5}{2}^+$, respectively, so that only $l=2$ is allowed. Even if one considers the possibility of spin-flip,^{13,14} and includes the effect of nonspherical boundary conditions,¹⁵ no $l=0$ is permitted.

Although it is common for simple stripping theory to disagree with experiment at small angles, the large discrepancy evident in Fig. 3 is most unusual. Moreover, the same reaction does not show any anomaly at a deuteron energy of 8.9 Mev⁵ (see Fig. 4). Careful checks were made to insure that no experimental errors were involved. The fact that the angular distribution for the 1.96-Mev level (Fig. 2), obtained at the same time, looks "normal," indicates that the scattering system was properly aligned. Data taken using nuclear emulsions to detect the analyzed protons (triangles in Fig. 3) confirm the electronic data. Finally, the possibility that some nucleus other than Mg^{24} was responsible for the high cross section at small angles was checked by bombarding several targets. One of these was made by depositing magnesium oxide powder, enriched to 99.7% in Mg^{24} , on a thin gold foil. This target was not very uniform, and the data points obtained with it (open circles in Fig. 3) show some scatter. The only nuclei lighter than calcium having known energy levels which might be undistinguishable from the Mg^{25} g.s. in our experiment are P^{32} and Cl^{36} . A target of chemically

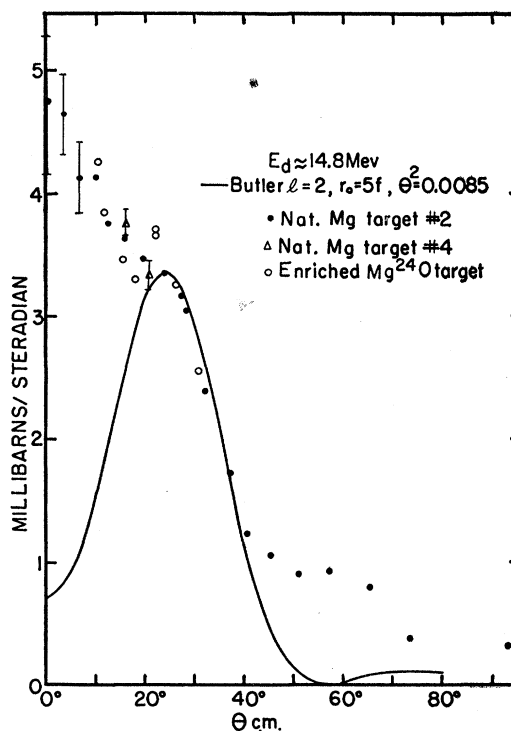


FIG. 3. Angular distribution for the $\text{Mg}^{24}(d,p)\text{Mg}^{25}$ g.s. reaction at $E_d \approx 14.8$ Mev. The filled circles represent data obtained with a metallic target of natural magnesium. The open circles were obtained from a powder target of enriched Mg^{24}O . The triangles were obtained from a separate run with a natural metallic target and were used to determine the absolute cross-section scale. The statistical errors are indicated for these two points. The statistical errors on all other points are less than 3% (and less than 2% for most of the closed circles). The errors shown for the points at the three lowest angles are due to inaccuracies of the beam monitor and are estimated errors.

pure magnesium carbonate, containing less than 0.001% of Cl and of PO_4 , was also bombarded. The results (not shown) agree with the distribution of Fig. 3. We conclude that the forward maximum in the angular

TABLE I. $\text{Mg}^{24}\text{-Mg}^{25}$ reduced widths, l and r_0 values.

Reaction	Final level	l	r_0 (10^{-13} cm)	θ^2 , present experiment	$\theta^2(d,p)^a$	$\theta^2(p,d)^b$	θ^2 , predicted ^c
$\text{Mg}^{24}(d,p)\text{Mg}^{25}$	g.s.	2	5.0	0.0085	0.0096		(0.0085)
	1.96	2	4.3	0.0031	0.0043		0.0018
$\text{Mg}^{25}(d,t)\text{Mg}^{24}$	g.s.	2	5.4	0.0085		0.0079	(0.0085)
	1.368	2	6.0	0.017		0.022	0.015
	4.122	2	6.0	0.0028			0.0018
	4.24	2	6.0	0.00075			
	7.60	(1)	(6.0)	(0.001)			

^a The reduced widths in this column are extracted in reference 12 from the data of reference 5.

^b The reduced widths in this column are extracted in reference 12 from the data of reference 7.

^c The reduced widths in this column, taken from reference 12, are those predicted by Eq. (3) in the present paper, normalized to the value 0.0085 for the g.s. transition.

¹² M. H. Macfarlane and J. B. French (to be published).

¹³ J. E. Bowcock, Phys. Rev. **112**, 923 (1958).

¹⁴ A. P. French, Phys. Rev. **107**, 1655 (1957).

¹⁵ J. Sawicki and G. R. Satchler, Nuclear Phys. **7**, 289 (1958).

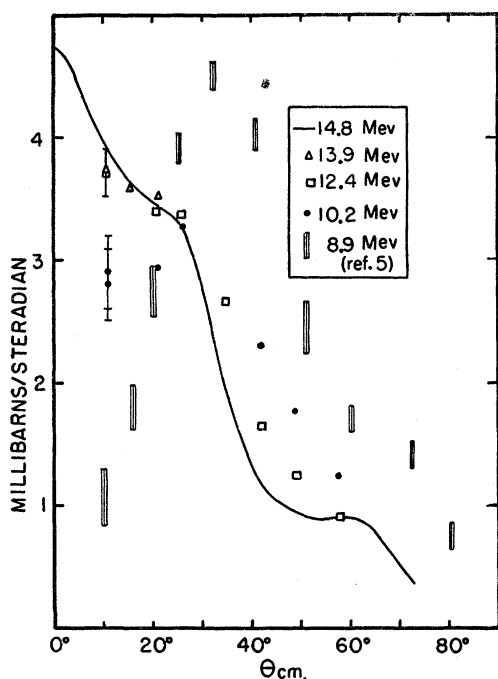


FIG. 4. Angular distribution for the $\text{Mg}^{24}(d,p)\text{Mg}^{25}$ g.s. reaction at several incident beam energies. The solid line is obtained from the data of Fig. 3 by drawing a smooth line through the experimental points. The results obtained with the beam energy degraded to ≈ 13.9 , ≈ 12.4 , and ≈ 10.2 Mev, and the results of Hinds *et al.*, reference 5, are also shown. The errors given are the statistical errors.

distribution is a property of the $\text{Mg}^{24}(d,p)\text{Mg}^{25}$ g.s. reaction at the deuteron energy of 14.8 Mev.

b. Results at Lower Energies

Because the results at $E_d = 8.9$ Mev show no anomaly in the angular distribution we decided to determine the energy dependence of the anomaly observed at 14.8 Mev. The incident deuteron energy was varied by inserting tantalum foils of different thicknesses in the beam path, ≈ 7 cm in front of the target. Collimating slits prevented deuterons scattered by more than 2° from reaching the target. The degraded beam had an energy spread of ≈ 200 kev at 12.4 Mev and ≈ 300 kev at 10.2 Mev (full width at half maximum).¹⁶

Figure 5 shows the proton spectra at three energies. At the lower energies the Mg^{25} g.s. group cannot be completely resolved from the groups corresponding to the Mg^{25} 0.58-Mev and Mg^{26} 3.97-Mev levels. Consequently, the Mg^{25} g.s. cross section cannot be determined as precisely as at full beam energy, particularly at small scattering angles where the Mg^{25} 0.58-Mev group is very intense. (At 10° it is ≈ 6 times as intense as the g.s. group.) However, the data are good enough to show whether there is a substantial change in the Mg^{25} g.s. cross section at small angles.

¹⁶ Details of the energy degrading method will be published elsewhere.

The results are given in Fig. 4, where the data of Hinds *et al.*⁵ are also reproduced. The inverse reaction $\text{Mg}^{25}(p,d)\text{Mg}^{24}$ has been studied in this energy region⁷ at a proton energy of 17 Mev, corresponding to $E_d = 11.9$ Mev. Bennett's⁷ angular distribution agrees with the 12.4-Mev data of Fig. 4 except at his smallest angle, $\theta_{c.m.} = 16^\circ$, where his data yield a cross section $\approx 75\%$ of the 29° cross section.

c. Discussion

The data of Fig. 4 show that at forward angles, $\theta < 30^\circ$, the cross section does not change appreciably with deuteron energy between 14.8 and 12.4 Mev, but decreases rapidly for lower energies until at 8.9 Mev there is a deep forward minimum in the angular distribution. At these angles the cross section obviously behaves very differently from the predictions of simple stripping theory, while for $\theta > 30^\circ$ the disagreement is not so great.

The theory predicts¹⁷ that the cross section should be a function only of the transfer momentum $q = |\mathbf{K}_p - (24/25)\mathbf{K}_d|$, where \mathbf{K}_p and \mathbf{K}_d are the wave vectors of the final and incident particles, respectively. Figure 6 shows the measured differential cross section plotted versus q . The 8.9-Mev data are again included, but have been normalized to the present data by multiplication by a factor 0.75; since the quoted error on the absolute cross sections of Hinds *et al.* and of the present experiment is $\pm 25\%$ for each, such a factor is consistent with the experiments.

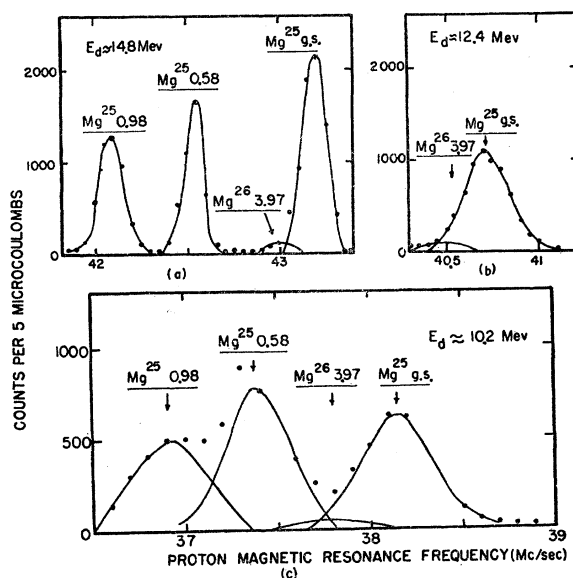


FIG. 5. Proton spectra from a natural magnesium target at $\theta_{lab} = 20^\circ$ at (a) full beam energy (14.8 Mev), and at two degraded energies, (b) 12.4 Mev, and (c) 10.2 Mev.

¹⁷ The factor K_p/K_d appears in the theoretical expression for the cross section, but this factor does not affect the relative angular distribution and will be neglected in the following discussion; it increases by $\approx 9\%$ when E_d decreases from 14.8 to 8.9 Mev.

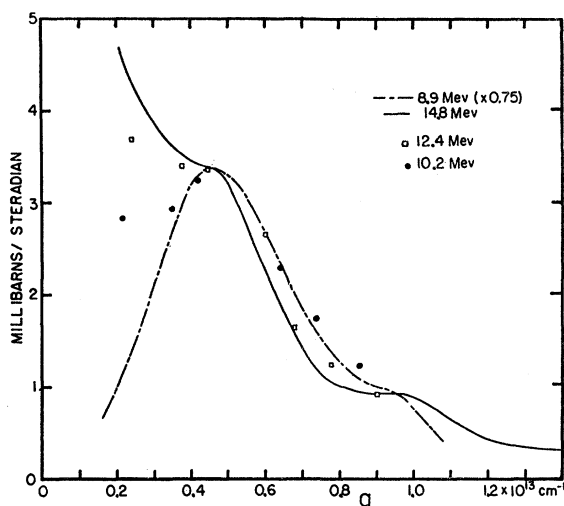


FIG. 6. Differential cross section for the $\text{Mg}^{24}(d,p)\text{Mg}^{25}$ g.s. reaction at several incident energies as a function of transfer momentum q . The solid line is obtained from the data of Fig. 3 by drawing a smooth line through the experimental points. The dashed line is obtained in a similar way from the data of Hinds *et al.* shown in Fig. 4, but the whole curve has been multiplied by a factor of 0.75.

The figure shows that agreement with theory is reasonable for $q > 0.4$, although the cross section at constant q seems to increase slightly with decreasing energy. The 10.2-Mev data agree within experimental error with the 8.9-Mev curve.

The behavior of the cross section at small angles shows that the reaction mechanism is more complex than that assumed in simple stripping theory, which is based on the plane-wave Born approximation. One possible explanation for the anomaly is that distortion effects are important. The distortion responsible for the effect may be in the deuteron wave function, in the proton wave function, or in both. It does not seem plausible that distortion of the deuteron wave is the important part. If it were, one might expect other proton groups produced by the same beam to show similar effects, yet the Mg^{25} 1.96-Mev level seems to have a normal angular distribution.

Another possible cause of the anomaly is interference between compound nucleus and direct reactions. To simulate such an interference, an attempt was made to fit the 14.8-Mev distribution by adding to the Butler stripping amplitude a partial wave whose amplitude and phase could be adjusted. It was found that the low-angle peak is no sharper than that obtained with the inclusion of an $l=2$ partial wave.

The $\text{Mg}^{25}(d,t)\text{Mg}^{24}$ g.s. reaction discussed in Sec. IV is a pickup reaction between the same two levels involved in the $\text{Mg}^{24}(d,p)\text{Mg}^{25}$ g.s. reaction. The (d,t) cross section also lies above the stripping curve at small angles (see Fig. 7), but the disagreement is much less striking than in the (d,p) case. This is not inconsistent with the idea that the anomaly is not due to a particu-

larity of the nuclear levels involved but is essentially a reaction mechanism effect.

Angular distributions similar to that of Fig. 3 have been observed previously, but have been interpreted as mixtures of $l=0$ and $l=2$. The present case is the only one in which the initial and final spins and parities are well known and are such as to forbid the mixture. However, it is possible that in some of the previous cases the forward maximum does not correspond to a mixture of $l=0$ and $l=2$ but to a reaction mechanism effect. To test whether the distribution is a true mixture, one could perform the experiment at several incident energies. For example, the $\text{Mg}^{25}(d,p)$ reaction to the 1.83-Mev level in Mg^{26} showed⁶ a distribution of the type in question at $E_d=8$ Mev; we are presently studying the reaction at $E_d \approx 15$ Mev.

It would be very interesting to obtain the angular distribution of the $\text{Mg}^{24}(d,p)\text{Mg}^{25}$ g.s. reaction out to 180° (at $E_d \approx 15$ Mev), to determine whether a back-angle peaking also occurs. One would also like to obtain at least the forward-angle distribution with more precision for deuteron energies between 10 and 14 Mev, and to extend the measurements to higher energies.

IV. $\text{Mg}^{26}(d,t)\text{Mg}^{24}$ REACTION

Triton angular distributions for eight states in Mg^{24} were obtained. A search for further states was made at $\theta_{\text{lab}} = 22^\circ$; one new level was found.

A. Experimental Results

a. $\text{Mg}^{25}(d,t)\text{Mg}^{24}$ g.s.

Figure 7 shows the angular distribution for this level. The Butler curve fits the data very well from 15° to 35° , but at small angles the experimental points lie far above the theoretical curve, as mentioned in the preceding section.

In order to extract absolute reduced widths from the data of (d,t) pickup reactions which can be compared to the reduced widths obtained from (d,p) stripping reactions, it is necessary to know the value of the triton normalization constant B^2 .⁴ This constant is chosen so as to make the reduced width of the Mg^{25} g.s. relative to the Mg^{24} g.s. core the same, whether it is extracted from the data for the $\text{Mg}^{25}(d,t)\text{Mg}^{24}$ reaction or for the $\text{Mg}^{24}(d,p)\text{Mg}^{25}$ reaction. The value obtained in the present experiment is $B^2 = 0.74 \times 10^{13} \text{ cm}^{-1}$.⁴ This value will be adopted for all (d,t) reactions described in the present article.

b. Other Levels

Angular distributions to the seven other states studied in this reaction are shown in Figs. 8 and 9. We have fitted with Butler curves those distributions which look somewhat like stripping curves. The corresponding reduced widths are given in Table I, column 5.

At $\theta_{\text{lab}} = 22^\circ$, we obtained a complete triton spectrum

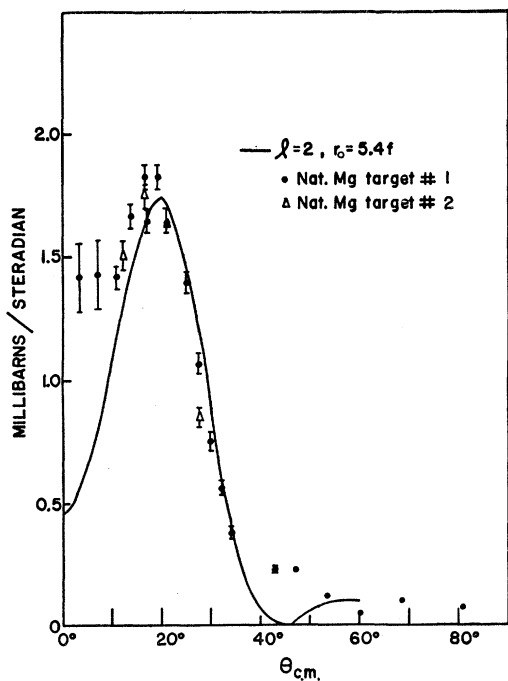


FIG. 7. Angular distribution for the $\text{Mg}^{25}(d,t)\text{Mg}^{24}$ g.s. reaction. The errors shown are statistical except at the two lowest angles where (as a result of the use of a different beam monitor) they are estimated upper limits on the errors.

for energies corresponding to Mg^{24} excitations from 4.1 to 7.6 Mev. This spectrum is shown in Fig. 10. The data points in the figure are counts recorded in the particular channel of the 6-channel pulse-height analyzer set to record scintillation pulses which had heights appropriate to reaction tritons appearing at the detector. There are background counts in this

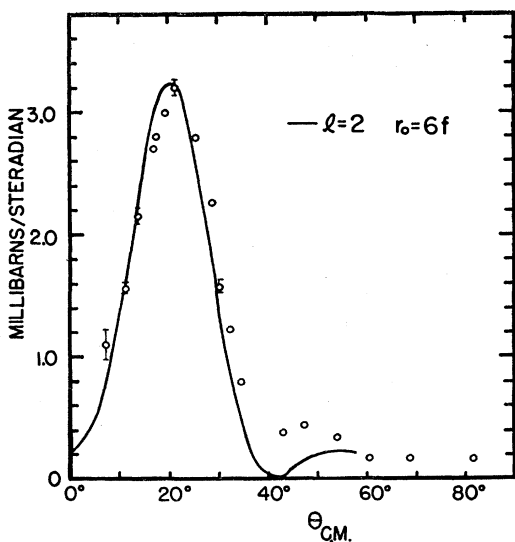


FIG. 8. Angular distribution for the $\text{Mg}^{25}(d,t)\text{Mg}^{24}$ 1.368-Mev reaction. Typical statistical errors are shown, except for the point at $\approx 7^\circ$, where the upper limit on the error is shown.

channel corresponding to deuterons which have lost energy by scattering inside the analyzing magnet. Other background counts occur because of anomalously small scintillator pulses produced by a small fraction of the deuterons elastically or inelastically scattered from various states of the target nuclei. Also, gamma rays produce a few pulses recorded in this channel.

These phenomena account for most of the constant background and for the larger count rates in the regions of Fig. 10 labeled *B*. For example, the relatively large count rate in the neighborhood of 44 Mc/sec is produced by deuterons from the intense $\text{H}^1(d,d)\text{H}^1$ scattering. The background at each point was determined from an analysis of the counts in the adjacent channels, and in every case of a suspected triton group a careful analysis also was made of the 256-channel analyzer data. Tritons could be recognized by their sharp pulse-height distribution ($\approx 10\%$ full width at half maximum).

We estimate that we would have identified any triton group having a cross section larger than 0.03 mb/sr. Several levels reported previously¹ between 4.3 and 7.3 Mev were not found. On the other hand, the level at 7.60 Mev has not been reported before.

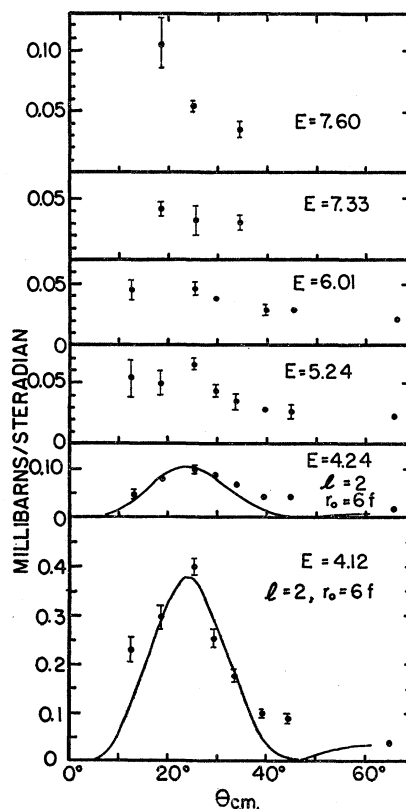


FIG. 9. Angular distributions for the $\text{Mg}^{25}(d,t)\text{Mg}^{24}$ reaction to the 4.12-, 4.24-, 5.24-, 6.01-, 7.33-, and 7.60-Mev levels. Typical statistical errors are shown. The distributions for the 4.12- and 4.24-Mev levels have been fitted with Butler curves. The 7.33- and 7.60-Mev distributions have too few points to fit, although an $\ell=1$, $r_0=6f$ curve is not inconsistent with the 7.60-Mev points. The remaining distributions cannot be fitted with Butler curves.

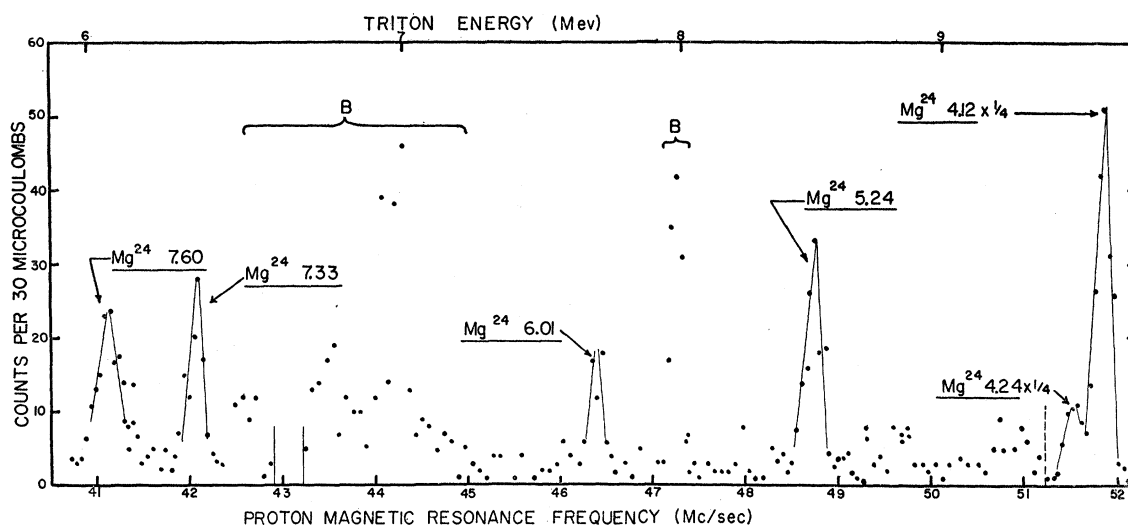


FIG. 10. Triton spectrum for the $\text{Mg}^{25}(d,t)\text{Mg}^{24}$ reaction at $\theta_{\text{lab}} = 22^\circ$, for triton energies corresponding to Mg^{24} excitations from 4.1 to 7.6 Mev. Most of the constant background is due to deuterons which have produced a pulse in the triton channel. In regions marked B the high count rate is due to an unusually high deuteron background. For example, the deuterons from the $\text{H}^1(d,d)\text{H}^1$ reaction account for most of the counts in the 2-Mc/sec region centered around 44 Mc/sec. The counts in the peak at 47.2 Mc/sec and (off scale) in the region between the vertical lines at ≈ 43 Mc/sec come from deuterons scattered within the analyzing magnet.

The excitation energies measured in the present experiment for the levels up through 5.24-Mev excitation agree with the values given by Endt and Braams.¹ For the three remaining levels, the energies and their estimated errors are, in Mev, 6.007 ± 0.020 , 7.330 ± 0.020 , and 7.600 ± 0.020 .

B. Discussion

As we have noted in Sec. I, the rotational model has been applied with success to the $A=25$ nuclei. Mg^{24} also has an approximately rotational spectrum; thus, it is natural to compare our experimental results with those predicted by the rotational model. Let us assume, then, that the Mg^{25} g.s. can be well described by the configuration shown in Fig. 11 in which the odd (13th) neutron is in Nilsson orbit^{18,19} No. 5 and all orbits below this one are filled, with the nuclear deformation parameter η having a value of ≈ 3 . From Fig. 11 it is clear that in the $\text{Mg}^{25}(d,t)\text{Mg}^{24}$ pickup reaction, only certain Mg^{24} states should be excited. By picking up the unpaired neutron in orbit No. 5 one would expect to reach only the Mg^{24} g.s. and the rotational states in the band based on the g.s. configuration. At somewhat higher excitation energies, one would expect to see the band based on the configuration of one neutron in each of orbits No. 5 and No. 7, as a result of the removal of a No. 7 neutron, and so on.

The reduced width θ^2 of a transition between states of two nuclei of masses A and $A+1$ can be written as a

product of two factors,

$$\theta^2 = S\theta_0^2. \quad (1)$$

The factor θ_0^2 is the single-particle reduced width.^{14,20}

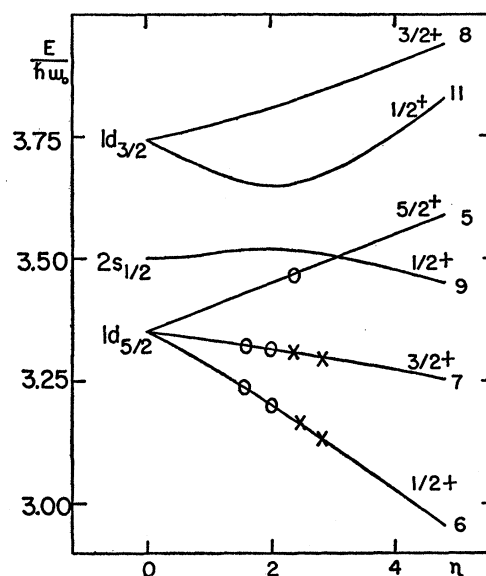


FIG. 11. Nilsson diagram for the Mg^{25} g.s. Only those orbits (numbered at the right of the diagram) arising from the $1d$ and $2s$ states are shown. The 12 protons (denoted by crosses) and the first 12 neutrons (denoted by circles) fill the Nilsson orbits up through No. 7; this is taken to be the g.s. configuration of Mg^{24} . The extra neutron of Mg^{25} is in orbit No. 5, so that the spin and parity of the Mg^{25} g.s. is $\frac{5}{2}^+$. The deformation parameter η has a value of ≈ 3 .

¹⁸ S. G. Nilsson, Kgl. Danske Videnskab. Selskab, Mat.-fys. Medd. 29, No. 16 (1955).

¹⁹ B. R. Mottelson and S. G. Nilsson, Kgl. Danske Videnskab. Selskab, Mat.-fys. Skrifter 1, No. 8 (1959).

²⁰ J. B. French, *Nuclear Spectroscopy*, edited by F. Ajzenberg-Selove (Academic Press, Inc., New York, to be published).

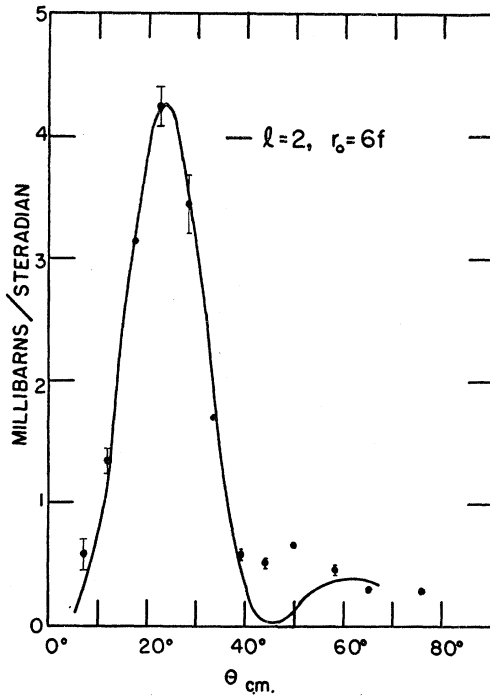


FIG. 12. Angular distribution for the $\text{Mg}^{26}(d,t)\text{Mg}^{25}$ g.s. reaction. Typical statistical errors are shown, except for the point at $\approx 7^\circ$, where the upper limit on the error is shown. The points are fitted with an $l=2$ Butler curve.

We assume in the present experiment that it has the same value for all transitions between two nuclei for which the transferred orbital angular momentum is the same. The spectroscopic factor S is given, for the rotational model, by^{14,21}

$$S_{lj} = \rho^2 \left(\frac{2J_0 + 1}{2J + 1} \right) (J_0 j K_0 \Omega | JK)^2 c_{lj}^2, \quad (2)$$

where J_0 is the angular momentum of nucleus A , J is the angular momentum of nucleus $A+1$, K_0 and K are the projections of the respective angular momenta along the nuclear symmetry axis, and j is the total angular momentum of the transferred nucleon, with a projection Ω along the symmetry axis. $\rho^2=2$ if either K or K_0 is zero, and is 1 otherwise. The Clebsch-Gordan coefficient $(J_0 j K_0 \Omega | JK)$ is a projection factor, occurring as a result of the nuclear rotation. The coefficients c_{lj} can be given in terms of coefficients tabulated by Nilsson¹⁸; c_{lj}^2 is then the probability for finding a nucleon with orbital angular momentum l and total angular momentum j in a given Nilsson orbit, and is a function of η .

In the present case of removal of the orbit No. 5 neutron from the even-odd target nucleus, the relative reduced widths to different levels within the rotational band differ only in the projection factors and the final

angular momenta. We have, from Eqs. (1) and (2),

$$\frac{\theta'^2}{\theta^2} = \left(\frac{2J_0' + 1}{2J_0 + 1} \right) \left[\frac{(J_0' \frac{5}{2} 0 \frac{5}{2} | \frac{5}{2} \frac{5}{2})^2}{(J_0 \frac{5}{2} 0 \frac{5}{2} | \frac{5}{2} \frac{5}{2})^2} \right], \quad (3)$$

where the primed and unprimed quantities refer to the two different states. In column 8 of Table I are shown the reduced widths predicted from Eq. (3) for the two excited states of the lowest rotational band, normalized to the g.s. reduced width of 0.0085. The agreement with the experimentally determined reduced width is good for the first (2^+) excited state, but for the second (4^+) excited state there is disagreement by a factor of 1.5, far outside the experimental uncertainty. This disagreement is probably a result of admixtures of states. Other evidence points to such admixtures, e.g., the ratio of the excitation energies of the 4^+ state and the 2^+ state is 3.01 instead of the predicted 10/3.

At higher excitation energies the states are weakly excited, but the 4.24- and the 7.60-Mev levels, in particular, show some anisotropy in their angular distributions. The first can be roughly fitted with an $l=2$ curve. In the second case there are too few experimental points to justify one's fitting a stripping curve, although an $l=1$, $r_0=6f$ curve fits the three points better than any other l -value curve; assuming such a fit, one obtains the reduced width shown in parentheses in Table I. Pickup transitions to these higher states indicate admixtures in the Mg^{25} g.s. or in the Mg^{24}

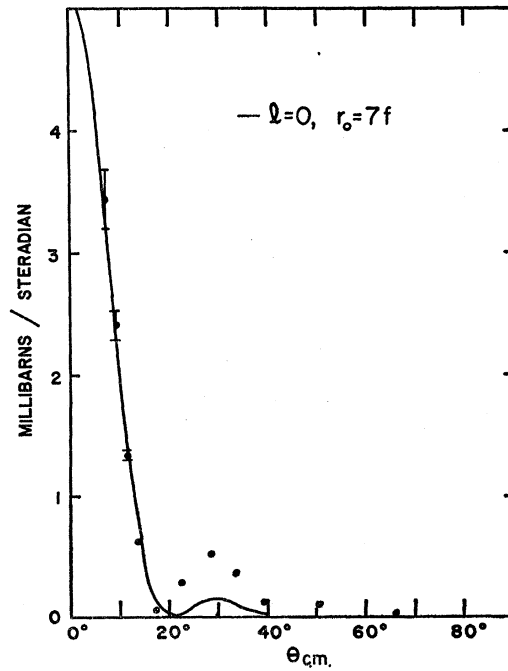


FIG. 13. Angular distribution for the $\text{Mg}^{26}(d,t)\text{Mg}^{25}$ 0.58-Mev reaction. Typical statistical errors are shown, except for the points at the two lowest angles, where the upper limits on the errors are shown. The points are fitted with an $l=2$ Butler curve.

²¹ G. R. Satchler, Ann. Phys. 3, 275 (1958).

TABLE II. $\text{Mg}^{26}(d, t)\text{Mg}^{25}$ reduced widths, and mixture probabilities of Nilsson configurations for the Mg^{26} ground state.

Level (Mev)	J^π	l	Nilsson orbit No.	$(\theta^2/\theta_0^2)_{\text{calc}}$		$(\theta^2)_{\text{exp}}$	$(\theta^2/\theta_0^2)_{\text{exp}}$	Mixture probability	
				$\eta = +2$	$\eta = +4$			$\eta = +2$	$\eta = +4$
g.s.	$5/2^+$	2	5	$2\alpha^2$	$2\alpha^2$	0.031	1.7	$\alpha^2=0.85$	$\alpha^2=0.80$
0.58	$3/2^+$	0	9	$1.3\beta^2$	$0.56\beta^2$	0.0025	0.11	$\beta^2=0.087$	$\beta^2=0.20$
0.98	$1/2^+$	2	9	$0.36\beta^2$	$0.92\beta^2$	0.0004	0.021	$\beta^2=0.058$	$\beta^2=0.023$
1.61	$5/2^+$	4	5	0	0		
1.96	$3/2^+$	2	9	$0.34\beta^2$	$0.52\beta^2$	0.0018	0.10	$\beta^2=0.29$	$\beta^2=0.19$
2.56	$1/2^+$	0	11	$0.39\gamma^2$	$0.94\gamma^2$	0.0007	0.032	$\gamma^2=0.082$	$\gamma^2=0.034$
2.80	$3/2^+$	2	11	$1.62\gamma^2$	$0.97\gamma^2$	0.0009	0.050	$\gamma^2=0.031$	$\gamma^2=0.052$

states themselves. Not enough is known about the higher excited states of Mg^{24} to permit further conclusions to be drawn from the data.

V. $\text{Mg}^{26}(d, t)\text{Mg}^{25}$ REACTION

A. Experimental Results

Triton angular distributions for eight levels in Mg^{25} are shown in Figs. 12, 13, and 14. A complete triton spectrum was obtained at $\theta_{\text{lab}}=25^\circ$ for triton energies corresponding to Mg^{25} excitations from 0.58 to 4.5 Mev; in addition to the eight states for which the angular distributions are shown, the 2.74-, 3.90-, 3.97-, and 4.05-Mev states were observed. The 3.90-, 3.97-, and 4.05-Mev levels were not well resolved; their cross sections appear to be of the same order of magnitude at this angle, and also at $\theta_{\text{c.m.}}=17.6^\circ$, where the combined cross section for the three levels is $0.09 \text{ mb/sr} \pm 15\%$.

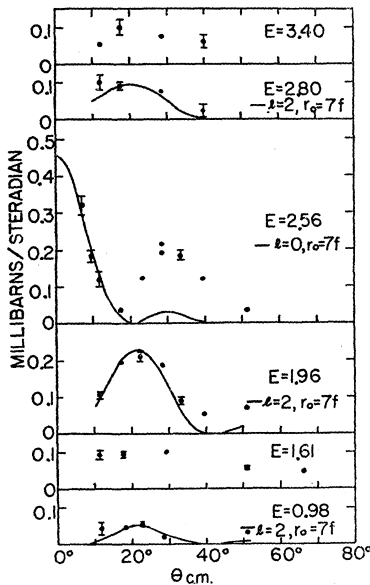


FIG. 14. Angular distributions for the $\text{Mg}^{26}(d, t)\text{Mg}^{25}$ reaction to the 0.98-, 1.61-, 1.96-, 2.56-, 2.80-, and 3.40-Mev levels. Typical statistical errors are shown, except for the points at the two lowest angles of the 2.56-Mev distribution, where the upper limits on the errors are shown. The distributions for the 0.98-, 1.96-, 2.56-, and 2.80-Mev states have been fitted with Butler curves; the distributions for the 1.61- and the 3.40-Mev states cannot be so fitted.

The 2.74-Mev level was not well resolved from the 2.80-Mev level, and appears to be much smaller than the latter at small angles. The largest cross section observed for the 2.74-Mev level was $0.030 \text{ mb/sr} \pm 20\%$, at $\theta_{\text{c.m.}}=28.6^\circ$. We estimate that in the survey at 25° any additional triton group having a cross section larger than 0.07 mb/sr would have been identified.

For each case in which the angular distribution looked somewhat like a stripping curve, the points were fitted with a Butler curve. Because the spin and parity of the Mg^{26} g.s. are 0^+ , and the spins and parities of all the observed Mg^{25} states are well known,² the l values of the transferred neutron are uniquely determined. From these curves the reduced widths were extracted, and are given in Table II, column 7.

B. Discussion

The pickup reaction from Mg^{26} to Mg^{25} yields information primarily on the wave function of the Mg^{26} g.s. Figure 15 shows the assignments of the low-lying states of Mg^{25} to various rotational bands based on Nilsson's orbits (Fig. 11), as made by Litherland

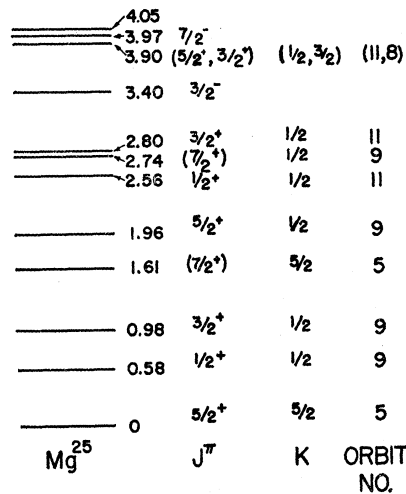


FIG. 15. Known low-lying energy levels of Mg^{25} . The spin and parity J^π of each state is shown. The value of K , the projection of J along the nuclear symmetry axis, is given in the next column, and the corresponding Nilsson orbit No. of the last neutron (see references 2 and 12) is given in the last column.

et al.,² and Macfarlane and French.¹⁴ The value of η is taken to be ≈ 3 . Using this model, one could then make the simple assumption that the g.s. wave function of Mg^{26} consists of two neutrons in orbit No. 5 with all orbits below this filled, the same value of η being appropriate. The prediction for the $\text{Mg}^{26}(d,t)\text{Mg}^{25}$ pickup reaction would then be that only the Mg^{25} g.s. and the rotational states based on this orbit could be formed. The fact that we observe pickup angular distributions for Mg^{25} states belonging to bands based on higher Nilsson orbits, in contradiction to this prediction, implies that there is band mixing in the Mg^{26} g.s.

A better approximation to the Mg^{26} g.s. wave function is to consider it as a mixture of three Nilsson configurations for the last two neutrons, i.e., both neutrons in orbit No. 5 (probability of α^2), both neutrons in orbit No. 9 (probability of β^2), and both neutrons in orbit No. 11 (probability of γ^2). One may write this wave function symbolically as

$$\text{Mg}^{26} \text{ g.s.} \equiv \alpha(\text{No. } 5)^2 + \beta(\text{No. } 9)^2 + \gamma(\text{No. } 11)^2. \quad (4)$$

Because the two neutrons must couple to spin zero, configurations in which only one of them is in orbit No. 5 are not allowed. The configuration in which one neutron is in orbit No. 9 and one in orbit No. 11 is allowed, however; we neglect it on the grounds that pairing effects favor configurations in which two neutrons are in the same orbit.²²

The experimental results allow the determination of α , β , and γ . Thus, for example, the reduced width for the transition to the Mg^{25} g.s. is $\theta^2 = \alpha^2 S_5 \theta_0^2(1d)$; for the transition to the Mg^{25} 0.58-Mev level it is $\theta^2 = \beta^2 S_9 \theta_0^2(2s)$; for the transition to the Mg^{25} 0.98-Mev level it is $\theta^2 = \gamma^2 S_{11} \theta_0^2(1d)$; and so on. Here, S is calculated for the appropriate transition from Eq. (2), using Nilsson's wave functions, and $\theta_0^2(2s)$ and $\theta_0^2(1d)$ are the single particle reduced widths for $l=0$ and $l=2$, respectively. One thus has the values of $(\theta^2/\theta_0^2)_{\text{calc}}$ given in columns 5 and 6 of Table II, in which we have calculated each S for $\eta=2$ and $\eta=4$. By equating each $(\theta^2/\theta_0^2)_{\text{calc}}$ to the corresponding $(\theta^2/\theta_0^2)_{\text{exp}}$, we obtain values for α^2 , β^2 , and γ^2 . We have chosen $\theta_0^2(1d)_{\text{exp}} = 0.018$ for the $\eta=2$ case in order to make the experimental and the calculated values of θ^2/θ_0^2 agree for the transition to the Mg^{25} g.s.²³ Macfarlane and French¹⁴ find, from an analysis of the $\text{Mg}^{24}(d,p)\text{Mg}^{25}$ reaction, that $\theta_0^2(2s)/\theta_0^2(1d) \approx 5/4$. We have adopted this ratio to obtain the results shown in the table.

In the discussion above, we have neglected rotation-particle coupling (RPC)²⁴ between the states in the

band based on orbit No. 9 and those in the band based on orbit No. 11. The coupling occurs because both these bands have $K = \frac{1}{2}$. An estimate of the amount of mixing produced may be made by using the relations given by Kerman²⁵; from this estimate one determines that, for the lower states in the bands, the values of β^2 and γ^2 are changed at most by a few percent, so that the neglect of RPC effects is justified for our purposes.

When the values of β^2 or γ^2 in Table II obtained from different levels of the same band differ from each other, this means that the relative reduced widths are not given correctly by our simple model. For example, the large value of β^2 obtained for the 1.96-Mev state is probably due to an admixture of orbit No. 5 in its wave function. This can occur through the interaction of this state with the g.s., which is also a $\frac{5}{2}^+$ state. A probability of 0.04 for this admixture would be sufficient to bring the value of β^2 extracted from the data for this state down to ≈ 0.1 . The values of β^2 and γ^2 for the lowest states ($J = \frac{1}{2}$) of the respective rotational bands are perhaps the most reliable. From them we extract the "most probable" values and estimated uncertainties,

$$\begin{aligned} \alpha^2 &= 0.83 \pm 0.05, \\ \beta^2 &= 0.13 \pm 0.05, \\ \gamma^2 &= 0.04 \pm 0.03. \end{aligned} \quad (5)$$

C. Pairing Energy

The admixtures found in the Mg^{26} g.s. show that, for this nucleus, it is not sufficient to consider a Hamiltonian of the type used by Nilsson. There is a perturbation of this Hamiltonian which produces the admixtures present in the g.s. wave function. We remark that rotation-particle coupling cannot be the responsible perturbation because RPC (in the first order) mixes only bands whose K 's differ by one, or have the value $\frac{1}{2}$. The admixture can, however, be due to a pairing energy; calculations with a pairing Hamiltonian have had considerable success in accounting for the properties of heavier nuclei,²⁶ and have also been considered for the light nuclei.²² We therefore attempt to account for the values of α , β , and γ given in (5) by using such a Hamiltonian.

We consider only the last two neutrons in Mg^{26} and neglect the possible excitations of the core of 24 particles; we also neglect the pairing energy between particles in different intrinsic states.²² Our set of basis states is obtained from the intrinsic spectrum of Mg^{25} , comprising the $\epsilon_1=0$ ($\frac{3}{2}^+$), $\epsilon_2=0.58$ -Mev ($\frac{1}{2}^+$), and $\epsilon_3=2.56$ -Mev ($\frac{1}{2}^+$) levels. Two particles can then be in four possible states: (a) both in the g.s., (b) both in the 0.58-Mev state, (c) both in the 2.56-Mev state, and (d) one in the 0.58-Mev state and one in the 2.56-Mev

²² D. M. Brink and A. K. Kerman, *Nuclear Phys.* **12**, 314 (1959).

²³ The value of 0.018 for $\theta_0^2(1d)$ is rather small. From the $\text{Mg}^{24}(d,p)\text{Mg}^{25}$ experiment, Macfarlane and French extract an average value of $\theta_0^2(1d) \approx 0.034$, while the $\text{Mg}^{24}(d,p)\text{Mg}^{25}$ g.s. data of Fig. 3 yield $\theta_0^2(1d) \approx 0.025$.

²⁴ A. K. Kerman, *Nuclear Reactions* (North-Holland Publishing Company, Amsterdam, 1958), Vol. 1, Chap. X.

²⁵ A. K. Kerman, *Kgl. Danske Videnskab. Selskab, Mat.-fys. Medd.* **30**, No. 15 (1956).

²⁶ L. S. Kisslinger and R. A. Sorensen (to be published).

state. Our Hamiltonian will be²⁶

$$H = \sum_{\substack{i=1,2,3 \\ p=\Omega(i), -\Omega(i)}} \epsilon_i a_{ip}^\dagger a_{ip} - G \sum_{j=1,2,3} a_{i\Omega(i)}^\dagger \times a_{i\Omega(i)}^\dagger a_{j\Omega(j)} a_{j\Omega(j)}, \quad (6)$$

where the $a_{i\Omega(i)}^\dagger$ and $a_{i\Omega(i)}$ are creation and annihilation operators, respectively, for a particle in orbit i whose angular momentum along the symmetry axis is $\Omega(i)$. The constant G measures the strength of the pairing energy; it has been assumed to have the same value for all orbits. The matrix of the Hamiltonian (6) in the representation of the four basis vectors (a), (b), (c), and (d) is

$$\begin{pmatrix} 2\epsilon_1 - G & -G & -G & 0 \\ -G & 2\epsilon_2 - G & -G & 0 \\ -G & -G & 2\epsilon_3 - G & 0 \\ 0 & 0 & 0 & \epsilon_2 + \epsilon_3 \end{pmatrix}. \quad (7)$$

The matrix (7) was diagonalized for various values of G . It was found that for $G \approx 0.6$ Mev the following admixture occurs in the ground state: $\alpha^2 = 0.82$, $\beta^2 = 0.16$, $\gamma^2 = 0.02$, in reasonable agreement with (5). This value of $G \approx 15/A$, where A is the mass number, is of the order of magnitude expected from the analysis of heavier nuclei; in the Pb region Kisslinger and Sorensen²⁶ find $G \approx 30/A$, and for $A \approx 60$ they find $G \approx 20/A$.

Other properties of the Mg^{26} nucleus do not agree, however, with the Hamiltonian (6) with $G = 0.6$ Mev. The spectrum of 0^+ levels prescribed by this Hamiltonian is shown in Fig. 16 for $G = 0$ and for $G = 0.6$ Mev. One sees that another 0^+ level is predicted at ≈ 1.8 Mev above the g.s., and that the g.s. is depressed by 0.97 Mev, for $G = 0.6$. Both features disagree with experiment: (a) No 0^+ level except the ground state is known in Mg^{26} , as can be seen from Fig. 16, which also shows the known spectrum up to 4.5-Mev excitation. (b) The binding energy of Mg^{26} relative to Mg^{24} is 18.45 Mev, and that of Mg^{25} is 7.33 Mev. The depression of the Mg^{26} g.s. due to pairing is therefore $18.45 - (2 \times 7.33) = 3.79$ Mev, and not the predicted ≈ 1 Mev.

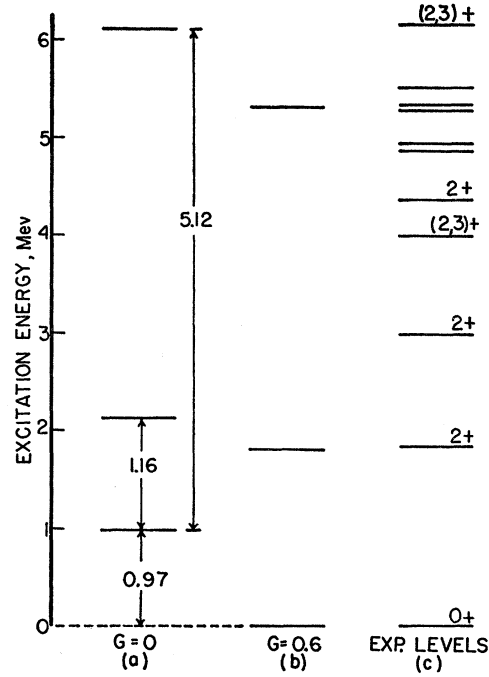


FIG. 16. Predicted 0^+ levels of Mg^{26} . (a) shows the relative positions of the g.s. and the first two excited 0^+ levels for a pairing energy parameter value of $G = 0$; (b) shows the same levels for $G = 0.6$. In column (c) the known levels of Mg^{26} , with their spins and parities, are shown for comparison.

Both disagreements (a) and (b) seem to call for a stronger pairing energy than $G \approx 0.6$ Mev, but a larger value of G would introduce too much admixture into the Mg^{26} g.s. It therefore appears impossible to account for the properties of Mg^{26} with such a simple model. A better treatment would probably take into account the excitations of the core.

ACKNOWLEDGMENTS

The authors wish to thank M. H. Macfarlane, R. A. Sorensen, L. S. Kisslinger, S. Meshkov, N. Austern, and J. C. Armstrong for helpful discussions, and A. J. Allen for his generous support.